Identification of winter storm contributions to snowpack in the Upper Colorado Basin

Mu Xiao[1] and Dennis P. Lettenmaier[1]

[1]Department of Geography, University of California, Los Angeles, CA

Corresponding author: Dennis P. Lettenmaier (dlettenm@ucla.edu)

Key Points:

- Apprioxmaitely 70% of the winter storms in the basin are affected by Atmospheric River and supply over half of the snow peak
- More minor snowfall events occur during dry and warm years but moderate and heavy storms are always the predominant source of SWE
- There is no significant trend on a basin-wide basis while some parts of the domain show regional upward trend

Abstract

We used the Variable Infiltration Capacity (VIC) macroscale hydrology model to reconstruct daily snowpack records in the Upper Colorado River Basin headwaters for the 67-water-year period 1949-2015 with focus on the accumulation season. We applied a snowfall-based storm identification method to the reconstructed data to attribute the sources of the accumulated snow as either Atmospheric River (AR) (based on an AR catalog) and non-AR. Over our study period, and using a definition based on basin-average snow water equivalent (SWE) increase, we find that there are on average 37.4 days during which snow accumulates each year, consisting of an average of 16.2 storms per water year. These storms account for an average of 78.2% of annual peak SWE. This number is higher (86.1%) in wet years than during dry years (70.3%). 69% of all storms on average are AR-related they contribute 56.3% of the annual snowpack peak. Although there are no significant basin-wide trends in AR-storm days or storm days per year over our study period, we found that there were parts of the basin (mostly in the middle latitudes) with significant upward trends in the contributions of AR-days and storms to accumulated SWE.

1. Introduction

The Colorado River is the largest river in the U.S. Southwest, and the region's most important surface water source. Although the area of the entire Colorado River Basin (CRB) is approximately 637,000 km^2, more than 90% of the natural streamflow is generated in the Upper Colorado Basin (UCRB) above Lees Ferry, AZ. The river is highly influenced by snowpack in the Rocky Mountain headwaters sub-basins, which account for over 70% of the river's annual flow (Li et al., 2017). The Colorado River is one of the most heavily regulated rivers in the world, owing to municipal and agricultural water demands in the Lower Basin (below Lees Ferry) where some 13,000 km^2 of agricultural lands are irrigated with river water (Cohen et al., 2013), and from which an additional ~20% of the river's flow is transferred to California for agricultural and urban water supply. The ability of the river to meet these water demands is aided by two large reservoirs, Lakes Powell and Mead, which have a combined storage capacity in excess of four times the mean flow at Lees Ferry. Given the exceptionally high use of the river's water and the need to efficiently manage it in the face of a warming climate, better understanding of the hydrological behavior and patterns within the basin are of great interest both to the scientific and water management communities.

Despite the significance of the snowpack in the UCRB headwaters, the long-term climatology of winter storm contributions to the snowpack have not been carefully explored. It is known that differences in climatic conditions strongly affect the snowpack variability over the mountainous parts of the UCRB (Trujillo & Molotch, 2014). Snow observations come mostly from the NRCS SNOTEL Snow Water Equivalent (SWE) network with about 80 stations across the UCRB, most of which have been in operation since the 1980s and 1990s, and predecessor manual snow course observations. Some previous studies have attempted to reconstruct the snowpack in the basin with a variety of data sources and tools. Schneider & Molotch (2016) used SNOTEL SWE data combined with Moderate Resolution Imaging Spectroradiometer (MODIS) satellite snow areal extent imagery to improve the real-time snowpack estimate in the Colorado River Basin. Timilsena & Piechota (2008) analyzed tree-ring chronologies for the period 1500-1980, and reconstructed SWE at a set of snow course sites in the UCRB. Several model-based experiments have also reconstructed snowpack over the UCRB. Barlage et al. (2010) improved the snow simulation in the Noah land surface model (Ek et al., 2003) and reported improved performance of the updated model's ability to simulate the magnitude and timing of seasonal maximum SWE over the UCRB headwaters. Ikeda et al. (2010) evaluated seasonal variations in UCRB snowpack using the Weather Research and Forecasting (WRF) regional climate model. The implications of future warming over the UCRB, including snowpack changes, were studied using WRF by Rasmussen et al. (2011). Chen et al. (2014) employed several well-known hydrological models to simulate SWE over the UCRB. However, none of the previous published work has evaluated the contribution of winter storms (and in particular, Atmospheric Rivers) to SWE in the UCRB.

In contrast, several recent studies have evaluated the characteristics of storms that contribute to snowpacks in the Sierra-Nevada (Dettinger, 2016; Eldardiry et al., 2019; Huning & Margulis, 2017; Margulis et al., 2016). These studies are potentially relevant to the UCRB as well, notwithstanding that there are important differences in winter storm patterns in the two regions. California winter precipitation is highly dependent on large storms, as the wettest 5% of precipitating days contribute around 1/3 of the total precipitation (Dettinger, 2016). Huning & Margulis (2017a) analyzed a high-resolution reanalysis SWE dataset (Margulis et al., 2015, 2016) for the Sierra Nevada and found that more than half of the snowpack in the region come from three or fewer large storms. They defined snowstorms as periods during which basin-wide SWE accumulates (grid cells at 90-m resolution higher than 75th percentile of the elevation distribution show positive SWE changes) with increases greater than 1% of the total annual maximum SWE (ΔSWE>1%). They found that at least 50% of the accumulated snow (averaged over the Sierra Nevada) comes from no more than three large storms. Eldardiry et al., (2019) used WRF reconstructions of hydroclimatic variables along the Pacific Coast of the western U.S. and found that high positive net snow accumulation during winter is mostly associated with AR events.

Here, we utilize the physically-based, semi-distributed Variable Infiltration Capacity (VIC) hydrological model forced with the Livneh et al. (2013) dataset to reconstruct SWE over the headwaters of the UCRB (Fig.1) for water years 1949-2014 (hereafter any reference to years implies water years unless stated otherwise). We then use the simulated SWE data to identify storms and assess their spatial patterns and origins, including storms (and storm days) that are associated with ARs.

2. Dataset and Methods

2.1 Hydrologic model and meteorological forcings

We used the Variable Infiltration Capacity (VIC) model (Liang et al., 1994) version 4.2.d as our primary tool to reconstruct snowpack over the UCRB during our 1949-2014 study period. We focused on the accumulation season, which we define as the period from Oct-1st to the date of domain-average peak SWE each water year, where we defined our domain as all 1/16th degree grid cells in the UCRB where long-term average Apr-1st SWE exceeded 50 mm (see Figure 1). The VIC model requires gridded meteorological variables as forcings. We used daily gridded records (at 1/16th degree spatial resolution) of precipitation, temperature maximum, temperature minimum, wind speed from the Livneh et al. (2013) data set (hereafter L13). We applied the Mountain Climate (MTCLIM) algorithm (see Bohn et al., 2013 for details) to produce downward longwave and shortwave radiation, surface air pressure and humidity.

2.2 Snow observation and AR catalogs

SNOTEL stations (of which there are 86 within our domain) collect daily SWE, air temperature, and precipitation observations dating back to the 1980s (and in some cases 1990s) over the Western U.S. The SWE observations reported at SNOTEL stations are measured by automated snow pillows which essentially weigh the overlying snow mass. The 86 SNOTEL sites we used all have data availability from 1991 or earlier. We downloaded all the available records for each of the 86 sites for further analysis.

We used the AR catalog of Guan & Waliser (2015) which is based on the NCEP-NCAR reanalysis. The AR catalog is derived from 6-hourly global atmospheric products from the NCEP/NCAR reanalysis (Kalnay et al., 1996) for calendar years 1948-2015 and has been used in other snow-related studies (e.g. Eldardiry et al., 2019; Goldenson et al., 2018; Huning et al., 2019; Little et al., 2019). Details of the detection algorithm and the AR catalog can be found in Guan & Waliser (2015) and therefore are not discussed here.

2.3 Storm identification

We followed the approach of Huning & Margulis (2017) which defines storms based on SWE volume with minor modifications. We categorized storm days as days with basin-wide average SWE increase equal or greater to 1% of the long-term average of the domain's annual SWE maximum (270 mm for our domain). We aggregated consecutive storm days into storms, which accounts for the possibility that snowfall events can be longer than one day (Serreze et al., 2001).

One concern about this identification approach is that it may miss storms that partially cover the domain. In order to address this issue, we tested a cell-based storm identification criterion, and then defined basin-scale storm days as occurring when more than 30% of the grid cells in our domain had SWE increases larger than the 2.7 mm threshold (1% of 270 mm) on the given day. The number of storms and AR-storms identified by the two methods are quite similar (less than 10% difference) as shown in Supplement Figure S1. The consistency of the two methods indicates that we are not missing major storms that cover only part of the domain. Therefore, we used the basin-average threshold in our subsequent analysis.

As we apply our identification algorithm, the storm identification threshold is a fixed value taken as the average over the entire domain (2.7 mm/d). We use this criterion to analyze spatial diversity of storm contributions to SWE across the domain, as well as the contributions in drought and wet years. Apart from identifying major snowfall events, we further classified storms into AR and non-AR categories using the Guan & Waliser (2015) catalog. For each storm identified as described above, we then checked whether an AR event occurred in the domain on the same date (as well as one day before and one day after). Following this approach, we classified all storms into AR-related and non-AR types for further evaluation.

3. Results and Discussion

3.1 Snowpack reconstruction verification

We used the VIC model to reconstruct the snowpack over our 67-year study period. The VIC model has been successfully applied in numerous previous studies of hydrological conditions and associated water resources of the Colorado River basin (e.g. Barnett et al., 2005; Barnett et al., 2008; Christensen et al., 2004; Christensen & Lettenmaier, 2007; Koster et al., 2010; Vano et al., 2012, 2014; Xiao et al., 2018; and others). More specifically, several previous studies have used the VIC model to address snow-related issues in the CRB. For instance, Mote et al. (2005, 2018) employed both in-situ measurements and VIC simulations to assess long-term snow declines in the mountainous Western U.S., and found that the trends estimated by the two approaches were in good agreement in the UCRB. For instance, Painter et al., (2010) examined the effects of dust radiative forcing on runoff responses in the UCRB using VIC model simulations. Deems et al., (2013), in a follow-up study, utilized the VIC model to estimate the combined influences of dust and regional warming on snowmelt and streamflow timing in the CRB. Li et al., (2017) performed VIC model simulations over the mountainous Western U.S. and used the results to evaluate the contribution of snowpack to annual streamflow across. In summary, the VIC model has been widely applied in the UCRB and elsewhere in the Western U.S. to reconstruct long-term variations in snowpack, in a manner similar to our application here.

The L13 data set likewise has been successfully used in a number of previous studies of the UCRB, including several of those mentioned above as well as Corringham & Cayan, 2019; Dierauer et al., 2018; Gautam & Mascaro, 2018; Hoerling et al., 2019; McAfee et al., 2019; and Yan et al., 2019. The L13 data set is observation (and model) based, and hydrologically consistent. It was derived from precipitation and temperature records from approximately 20,000 NOAA Cooperative Observer (COOP) stations across the conterminous U.S. It is an update an extension of the Maurer et al. (2002) data set. The methods used in the L13 data set are based on Maurer et al., (2002) but with higher spatial resolution and longer temporal coverage.

Notwithstanding the widespread use of the VIC model and the L13 data set, we evaluated the performance of both the model and data set. We extracted daily precipitation records during the accumulation season of each water year for all 86 of the SNOTEL sites (see Figure 1 for locations) as well as the L13 temperature and wind speed data to run the VIC model. The purpose of utilizing SNOTEL observed precipitation is to reduce the inconsistency between SNOTEL (point) and gridded values, as well as the effects of topographic differences between point observations and interpolated gridded data. Figure 2 shows the cumulative distribution functions (CDFs) of VIC-simulated and observed annual SWE maxima for 1991-2011. CDFs of average results over all sites and observed SWE peak values at five individual stations, which are geographically distributed across the domain (see Figure S2 and Table S1), are included in Figure 2. The simulated and observed CDFs of SWE annual peak values are within the same range, while the observations are generally slightly higher than VIC (the average difference in the median is 54.8 mm, 12.3% of the mean). The differences are likely due in substantial part to the fact that the VIC simulations are for an entire 1/16˚ grid cell and SNOTEL observations are for points within the grid cell. We also compared the time-series of the mean observed and simulated SWE values across the 86 SNOTEL sites (and the $1/16^{th}$ degree grid cells within which they lie) during the accumulation seasons (Figure S3) and the simulated results and the observed snow daily records agree quite well. On the basis of these comparisons, we conclude that the model results provide plausible reproductions of the observations, and should be sufficient for our purposes.

3.2 Basin-wide storm contribution

We applied the methods described in Section 2.3 to produce VIC-simulated SWE records using the L13 forcings to identify storms responsible for substantial SWE increases and the subset of those storms that are AR-related. Figure 3 shows time series plots of individual storm days, number of storms and number of AR-related storms. Over the entire study period, there were on average 37.4 storm days per year. The mean number of storms was 16.2 per year of which 69% (11.2) were AR-related.

After identifying the storms in each accumulation season, we calculated each storm's contribution to basin peak SWE for that water year. Figure 4 shows the contribution of storms to annual maximum SWE. We also show the contributions from each AR storm in the same figure. We note that we only include storm days within the AR-window (as described in section 2.3) in our calculation of AR-storm contributions (we use the same term "AR-storm" hereafter to denote the storm days within the AR-window). This definition is different from "AR-related" storms, although the difference is rather limited (only 10% of the storm days belonging to an AR-related storm are outside the AR-window). Finally, we calculated the contributions from all days when precipitation yielded SWE increases (denoted as "all precipitation" hereafter) in the accumulation season (Figure 4). In some cases, the estimates can exceed 100%. This can occur because we compared the accumulated precipitation to annual peak SWE over the entire domain, and some (low-elevation areas in particular) can experience mid-season melt. Furthermore, sublimation is a factor that results in accumulated precipitation exceeding annual peak SWE.

We find that the average contribution of AR-storms to annual peak SWE is 63.3% over the entire record, and the average contribution from all storm days is 78.2%, which indicates that a large portion (~80%) of the SWE in the UCRB originates from moderate to heavy snow storms. Huning & Margulis (2017) used a similar approach to estimate the range of snowstorm contributions in the Sierra-Nevada and found a range of 83%-93%. Compared to the Sierra Nevada, the values are smaller in the UCRB (perhaps because the distance from the coast is greater, and storms are somewhat less structured than in the Sierra Nevada) but nonetheless is still quite high. We also find that about 75% of all individual storm days are AR-related, and they produce 63% of the total maximum snow accumulation. The average contribution of all precipitation days to the grid cell maximum accumulation averaged over all grid cells in our domain is 116.8%, which implies that the excess (16.8% of the SWE maxima) melts (or is sublimated) before the domain's peak SWE occurs.

3.3 Wet, dry, warm and cold years

We selected the 10 most extreme years in each category (wet, dry, warm and cold) and investigated the contributions of storm days in each of these categories to SWE. We defined wet, dry warm, and cold based on the total precipitation amount or average temperature during the accumulation season (from Oct 1st to the date of peak SWE) averaged over our domain. Table 1 reports the annual average number of storm days, storms and AR-storms in each category. The number of storms and storm days (both AR and non-AR) is higher during wet and cold years compared with dry and warm years. The differences between the number of AR-storms in each of the extreme climatic categories are relatively small, given the fact that only about 10 AR-storms occur per year on climatological average. However, the differences in terms of storm days are larger – 54.9 vs. 23.0 days per year for wet vs dry, and 41.5 vs 36.2 cold vs warm, respectively.

Table 2 gives the percent contributions from storms and precipitation days to the maximum annual SWE for the four climatic categories, as well as the climatology (all years). Comparison of the statistics in wet and dry years suggests that while storms play a more important role in snow accumulation during wet years, the contribution percentages from all precipitation in wet years are nonetheless lower than for dry years. The reason for this is that the actual amount of accumulated SWE is much smaller during dry years, which makes contribution percentages rise. The SWE losses (difference between total accumulated SWE and the annual maxima) are similar for wet (2.4 km^3/yr) and dry (2.6 km^3/yr) years (but as a percentage of peak SWE, much larger in dry years). These results suggest that during dry years, relatively small snowfall events are more important to the accumulated snowpack in UCRB. Nonetheless, the dominant contribution to SWE is from storms in both wet and dry years. During dry years, not only are there are fewer storms, but the precipitation amount per storm also is less. The average SWE increase is 0.76 km^3 per storm for dry years and 1.57 km^3 per storm for wet years (reported in Table 2). On the other hand, the contribution percentages of AR-storms, all storms and all precipitation days are all higher in warm years than cold ones, and the accumulated maximum SWE decreases in warm years. The contribution from all precipitation in cold years are lowest as expected, arguably the result of less mid-season SWE loss by melt or sublimation (only 1.8 km^3/yr, 4% of the climatology in cold years, is eliminated during the mid-season). In cold and wet years, snowfall contributes more efficiently to maximum SWE (less midwinter loss) and the contributions from storms are higher (including AR storms). The flip side of that is that in warm and dry years, more of the total snowfall comes from minor events. Overall, 72.7% of all storms' contribution to annual peak SWE is attributed to AR-storms in all years, as high as 76.5% for wet years but still 70.7% in dry years (5^{th} row in Table 2).

Figure 5 shows the same bar plots as Figure 4 with wet and dry years highlighted. We estimated the distribution of the contributions to peak SWE for all the 67-year-long records using Weibull plotting positions (see Figure 5). Based on the plots of the contributions, we notice that generally both AR and non-AR storm contributions tend to be higher in wet years and lower in dry years. For the contribution of all precipitation, the results are somewhat different: the contributions (of storms to peak SWE) tend to be higher in dry years and lower in wet years. The reason for dry years having a higher contribution percentage is that maximum SWE in those years is small. More mid-season SWE loss in dry years also has some effect, but the main difference between dry and wet years (with respect to mid-season snowpack loss) is not large enough (2.7 vs 2.2 km^3/yr) to be the dominant cause.

Similar to Figure 5, Figure 6 shows the same information for warm and cold years. During warm years, because mid-season SWE loss effect is the largest amongst the four climatic conditions, the average percentages are high for AR-storm, all storm, and all precipitation. On the other hand, both the numbers in Table 2 and the distribution plots in Figure 6 show that storm contributions during cold years are not much smaller than for all years. This suggests that although lower winter temperatures result in greater snow accumulation (as the last row of Table 2 indicates), the percentage contribution from storms is not substantially affected. The major sources of SWE accumulation are still snowfall during storms and thereby are determined primarily by precipitation amounts.

3.4 Spatial analysis

Although we defined storms as basin-wide events, most storms do not cover the entire domain. Therefore, for all event measures (storms, AR-storms and storm days) we performed an analysis of SWE changes at each grid cell to determine whether that specific grid cellcontributed to particular events. If the grid cell's SWE increased by over 0.5 mm after the event (ΔSWE>0.5 mm), we considered that grid cell to have contributed to the event. Applying this 0.5 mm threshold for all the events, we determined each storm's coverage and number of events that each grid cell experienced. Using this measure, we found that on average, each storm affected 84.9% of the entire domain and each AR-storm affected 85.7% of the domain, which indicates that the AR-storms' scale is very similar to non-AR storms, but most cover a large part of the domain. Figure 7 shows the cumulative contribution of (AR-) storms (y-axis) as a function of storm cover fraction (x-axis), i.e. given a certain value, μ, the y-axis reports how much SWE is provided by

(AR-) storms that cover less than μ of the domain. Of all the contribution from AR-storms to annual peak SWE, 71.7% is attributable to AR-storms that affect more than 90% of the entire region. The contribution from AR-storms that cover less than 70% of the domain is only 6.2%. The remaining 22.1% (100%-71.7%-6.2%) is contributed by AR-storms that cover between 70-90% of the domain. If we perform the same calculation for all storms, we find that storms that cover at least 90% of the entire basin provide 67.9% of all storms' contribution to the SWE annual maxima. Storms that cover less than 70% of the basin yield 6.1% of the total contribution, which means the remaining 26.0% is attributed from storms that cover 70-90% of the domain. In summary, the contributions of both AR- and all storms are mainly attributable to events that cover much of the domain.

Figure 8 shows the multi-year average number of AR-storms, all storms and storm days on a grid cell basis averaged over the entire record (note that, as in Figure 1, we only consider grid cells with > 50 mm average Apr-1st SWE). We also show sub-basin boundaries for reference (more detailed information about the sub-basin analysis is included in the Supplement). In general, Figure 1 shows that on average. the eastern part of the basin has more storms and storm days than the western part of the basin. Furthermore, grid cells with more storm days also have higher snow accumulation (see Figure 1). Notwithstanding the west to east trend, spatial variations in storm statistics across the domain generally are modest.

If we compute ΔSWE for each event divided by the basin average peak SWE for each year, we can form a time series of the contribution of that grid cell to the basin's total snowpack. We do so in Figure 9, which shows the average contributions (over the entire study period) from AR-storms, all storms and all precipitation to basin total snowpack in each grid. The AR-storm (Fig.9 left panel) and storm (Fig.9 middle panel) maps generally show consistent spatial patterns:

the highest numbers are in the east and the smallest contributions are the grid cells with lowest SWE climatology (see Figure1). Nonetheless, if we take all precipitation into consideration, the northwestern part of the domain (around 42.5˚N) also makes large contributions to the basin snowpack (Figure 9 right panel). Because the number of storms days in the northwestern part of the basin are smaller than in the eastern part (Figure 8 right panel), the high contribution in the plot illustrate that small-scale snowfall events play a greater role in that (northwestern) part of UCRB than elsewhere.

We also extracted average AR-storm, storm and all precipitation contributions for warm and cold years (defined as described in section 3.3), results of which are shown as spatial maps in Figure 10. Figure 11 shows similar information but for wet and dry years. The spatial patterns of AR-storm and all-storm contributions during wet and cold years are mostly similar to the long-term climatology (Figure 8), where larger contributions tend to occur in those cells with more events. The northwest part (~42.5˚N) of the basin shows uncommonly high snowfall contributions (as do cool or wet years), which indicates that for warm and dry conditions minor snowfall events still are especially important as compared with the rest of UCRB.

3.5 Trend analysis

We performed the non-parametric Mann-Kendall (MK) test (Mann, 1945; Kendall, 1957) on the time series of basin-wide number of AR-related storms, all storms and number of storm days per year and found no trends at the 0.05 significance level. Further, the contributions of AR-storm, all storms and all precipitation reported in Figure 4 also failed to pass the MK-test at the 0.05 significance level. As for the basin-wide analysis, we found no trends in either the number of storms or SWE per storm, and for either AR- or all storms. In summary, we detected no statistically significant trends at the 5% significance level for the 1949-2015 period. However, we did find some statistically significant trends when we included earlier (pre-1949) SWE simulations. For instance, we tested the annual trends in number of storm days and storms over a longer period, 1916-2015, using VIC SWE output generated using the same methods (AR-related trends cannot be extended because the AR catalog is not available before 1948). The annual time series of both are show downward trends, which suggests that there are fewer storms in recent decades compared to the early 1900s. Nonetheless, the storms' annual contribution percentage to peak SWE does not show any (decreasing) trend over 1916-2015 as does the storm number, which suggests that the average contribution percentage per storm might be increasing. However, we checked the trend in ΔSWE per storm and found that there is no significant trend over the same period as above. Therefore, it appears that the increasing contribution percentage per storm must be the result of decreasing annual peak SWE (which in fact has been observed by others, see e.g. Mote et al., 2018; Xiao et al., 2019, and others).

We then applied the MK-test at each grid cell in the domain to evaluate the spatial pattern of trends. Figure 12 shows the grid cells with statistically significant trends in the number of AR-storms, storms and storm days. There are only 4.6% and 8.4% of total valid cells (long-term Apr 1st SWE > 50 mm) that have downward trends in the number of AR-storm and all-storms trends. The numbers of cells diagnosed as showing upward trends in the domain are negligible: no annual upward trend detected in AR-storms, one cell for number of all storms and four cells for number of individual storm days. Overall, the number of events in the basin does not show obvious trends over the study period as Figure 12 shows.

Although there are no statistically significant trends in any of the basin-average storm contributions (AR-storm, all-storm, and all precipitation), a number of individual grid cells in the domain have statistically significant trends as shown in Figure 13. The percentage of each type are summarized in Table 3. The grid cells with increasing contributions are primarily in the middle-latitude zone of the domain. In the northwest and southeast part of the domain, ~10% of the total cells have a significant downward trend in contributions of AR-storm, all-storm and all precipitation to the snowpack. Figure 14 shows the trend detected by the MK-test in temperature and precipitation during the accumulation season over all years. The spatial patterns in Figure 13 panel (b) and (c) match well with the pattern of trends in precipitation (Figure 14 right panel), which suggests that trends in precipitation likely are the primary factor. These maps suggest that over the entire study period, the snowpack source has moved (slightly) towards the mid-zone of the domain from the northern and southern extremes.

Finally, we applied field significance tests to investigate whether the trends detected at each individual cell are statistically significant at the domain level. We followed the approach proposed by (Livezey & Chen, 1983) in conducting field significance tests. We determined the degree of freedom (number of independent sites) following the Chi-square-distribution method proposed by (Wang & Shen, 1999). The results show that there are too few cells with trends in number for all three types of events (see Figure 12 presents) to pass the field significance test. However, the percentage of cells with trends in contributions are large enough (Figure 13) to be field significant. The fact that the basin-average results do not show statistically significant trends (discussed above) may be the result of upward and downward cells cancelling over the domain.

4. Summary and Conclusions

We applied the VIC model forced with the L13 dataset to reconstruct snowpack in the UCRB for the last six decades. On average, the simulated daily SWE time series successfully capture the major characteristics of surface observations during the accumulation season. Using the reconstructed SWE and meteorological data, we employed a snowfall-oriented definition to identify storm contributions to SWE and further investigate the storms variations and contributions over the domain. Specifically, we conclude that:

1. The average number of days identified as being associated with snowfall storms is 37.4 per year, consisting of an average of 16.2 storms that contribute to the majority (78.2%) of the annual peak SWE. Atmospheric Rivers in the UCRB affect ~70% of these storms and supply 56.9% of the accumulated snowpack's peak value. Compared to the Sierra Nevada region (Huning & Margulis, 2017), the values are smaller in the UCRB but nonetheless are still quite high.
2. In the mountainous parts of the UCRB, moderate and heavy storms are the predominant source of SWE for all four climatic conditions we studied. In wet and cold years, snowfall contributes more efficiently to annual peak SWE because the effects of mid-season melt and sublimation are smaller. More minor snowfall events occur under dry and warm scenarios, and they contributed to 48.4% and 35.8% peak SWE value during the accumulation season (compared with 21.0% and 27.6% during wet and cold years).
3. The eastern part of the basin tends to have more storms (and AR-storms) and higher storm contributions to snow accumulation than the western part. Small-scale snowfall events have the greatest effect on snow accumulation in the northwestern part of the basin. By investigating the coverage and contribution of each AR- and non-AR storm, we found that ~70% of the storms contribution to SWE is attributable to events that cover at least 90% of the domain. In other words, of all the (AR-) storms, domain-wide events make the main contribution to SWE.

4. On a basin-wide basis, there are no statistically significant trends in the total number of storms, number of AR-storms, or in total storm days over the 1949-2015 period for which AR information is available. However, the number of storms does show a statistically significant downward trend over a longer period (1916-2015). On the other hand, there are statistically significant trends for some (less than 1/3 of total number) individual grid cells. Upward trends mainly are in the mid-latitude mountainous portion of the basin and grid cells with downward trends are mostly in the northwestern and southeastern portions of the basin.

Acknowledgments

Support for this work was provided in part by Grant No. NA17OAR4310146 from NOAA's Modeling, Analysis, Predictions, and Projections Program. The data used in this study is archived as **https://doi.org/10.6084/m9.figshare.12152166.v1**.

References

Barlage, M., Chen, F., Tewari, M., Ikeda, K., Gochis, D., Dudhia, J., et al. (2010). Noah land surface model modifications to improve snowpack prediction in the Colorado Rocky Mountains. *Journal of Geophysical Research Atmospheres*, *115*(22), 1–15. https://doi.org/10.1029/2009JD013470

Barnett, T. P., Adam, J. C., & Lettenmaier, D. P. (2005). Potential impacts of a warming climate on water availability in snow-dominated regions. *Nature*, *438*(7066), 303–309. https://doi.org/10.1038/nature04141

Barnett, Tim P, Pierce, D. W., Hidalgo, H. G., Bonfils, C., Santer, B. D., Das, T., et al. (2008). Human-Induced Changes United States. *Science*, *319*(February), 1080–1083. https://doi.org/10.1126/science.1152538

Bohn, T. J., Livneh, B., Oyler, J. W., Running, S. W., Nijssen, B., & Lettenmaier, D. P. (2013). Global evaluation of MTCLIM and related algorithms for forcing of ecological and hydrological models. *Agricultural and Forest Meteorology*, *176*, 38–49. https://doi.org/10.1016/j.agrformet.2013.03.003

Chen, F., Barlage, M., Tewari, M., Rasmussen, R., Jin, J., Lettenmaier, D., et al. (2014). Modeling seasonal snowpack evolution in the complex terrain and forested colorado headwaters region: A model intercomparison study. *Journal of Geophysical Research*, *119*(22), 13795–13819. https://doi.org/10.1002/2014JD022167

Christensen, Nadia S, & Lettenmaier, D. P. (2007). A multimodel ensemble approach to assessment of climate change impacts on the hydrology and water resources of the Colorado River Basin. *Hydrology and Earth System Sciences Discussions*, *11*(4), 1417–1434.

Christensen, Niklas S., Wood, A. W., Voisin, N., Lettenmaier, D. P., & Palmer, R. N. (2004).

The effects of climate change on the hydrology and water resources of the Colorado River basin. *Climatic Change*, *62*(1–3), 337–363. https://doi.org/10.1023/B:CLIM.0000013684.13621.1f

Cohen, M., Christian-Smith, J., & Berggren, J. (2013). *Water to Supply the Land: Irrigated Agriculture in the Colorado River Basin*. Retrieved from http://water.usgs.gov/watercensus/colorado.html

Corringham, T. W., & Cayan, D. R. (2019). The effect of El Niño on flood damages in the western United States. *Weather, Climate, and Society*, *11*(3), 489–504. https://doi.org/10.1175/WCAS-D-18-0071.1

Deems, J. S., Painter, T. H., Barsugli, J. J., Belnap, J., & Udall, B. (2013). Combined impacts of current and future dust deposition and regional warming on Colorado River Basin snow dynamics and hydrology. *Hydrology and Earth System Sciences*, *17*(11), 4401–4413. https://doi.org/10.5194/hess-17-4401-2013

Dettinger, M. (2016). Historical and Future Relations Between Large Storms and Droughts in California. *San Francisco Estuary and Watershed Science*, *14*(2). https://doi.org/10.15447/sfews.2016v14iss2art1

Dierauer, J. R., Whitfield, P. H., & Allen, D. M. (2018). Climate Controls on Runoff and Low Flows in Mountain Catchments of Western North America. *Water Resources Research*, *54*(10), 7495–7510. https://doi.org/10.1029/2018WR023087

Ek, M. B., Mitchell, K. E., Lin, Y., Rogers, E., Grunmann, P., Koren, V., et al. (2003). Implementation of Noah land surface model advances in the National Centers for Environmental Prediction operational mesoscale Eta model. *Journal of Geophysical Research*, *108*(D22), 8851. https://doi.org/10.1029/2002JD003296

Eldardiry, H., Mahmood, A., Chen, X., Hossain, F., Nijssen, B., & Lettenmaier, D. P. (2019). Atmospheric River–Induced Precipitation and Snowpack during the Western United States Cold Season. *Journal of Hydrometeorology*, *20*(4), 613–630. https://doi.org/10.1175/jhm-d-18-0228.1

Gautam, J., & Mascaro, G. (2018). Evaluation of Coupled Model Intercomparison Project Phase 5 historical simulations in the Colorado River basin. *International Journal of Climatology*, *38*(10), 3861–3877. https://doi.org/10.1002/joc.5540

Goldenson, N., Leung, L. R., Bitz, C. M., & Blanchard-Wrigglesworth, E. (2018). Influence of atmospheric rivers on mountain snowpack in the western United States. *Journal of Climate*, *31*(24), 9921–9940. https://doi.org/10.1175/JCLI-D-18-0268.1

Guan, B., & Waliser, D. E. (2015). Detection of atmospheric rivers: Evaluation and application of an algorithm for global studies. *Journal of Geophysical Research: Atmospheres*, *120*(24), 12514–12535. https://doi.org/10.1002/2015JD024257

Haddeland, I., Lettenmaier, D. P., & Skaugen, T. (2006). Effects of irrigation on the water and energy balances of the Colorado and Mekong river basins. *Journal of Hydrology*, *324*(1–4), 210–223. https://doi.org/10.1016/j.jhydrol.2005.09.028

Haddeland, I., Heinke, J., Biemans, H., Eisner, S., Flörke, M., Hanasaki, N., et al. (2014). Global water resources affected by human interventions and climate change. *Proceedings of the National Academy of Sciences of the United States of America*, *111*(9), 3251–6. https://doi.org/10.1073/pnas.1222475110

Hamlet, A. F., & Lettenmaier, D. P. (2005). Production of Temporally Consistent Gridded Precipitation and Temperature Fields for the Continental United States. *Journal of Hydrometeorology*, *6*(3), 330–336. https://doi.org/10.1175/JHM420.1

Hoerling, M., Barsugli, J., Livneh, B., Eischeid, J., Quan, X., & Badger, A. (2019). Causes for the Century-Long Decline in Colorado River Flow. *Journal of Climate*, 8181–8203. https://doi.org/10.1175/jcli-d-19-0207.1

Huning, L. S., & Margulis, S. A. (2017). Climatology of seasonal snowfall accumulation across the Sierra Nevada (USA): Accumulation rates, distributions, and variability. *Water Resources Research*, *53*(7), 6033–6049. https://doi.org/10.1002/2017WR020915

Ikeda, K., Rasmussen, R., Liu, C., Gochis, D., Yates, D., Chen, F., et al. (2010). Simulation of seasonal snowfall over Colorado. *Atmospheric Research*, *97*(4), 462–477. https://doi.org/10.1016/j.atmosres.2010.04.010

Kalnay, E., Kanamitsu, M., Kistler, R., Collins, W., Deaven, D., Gandin, L., et al. (1996). The NCEP/NCAR 40-Year Reanalysis Project. *Bulletin of the American Meteorological Society*, *77*(3), 437–471. https://doi.org/10.1175/1520-0477(1996)077<0437:TNYRP>2.0.CO;2

Kendall, M. G. (1957). Rank Correlation Methods. *Biometrika*, *44*(1/2), 298. https://doi.org/10.2307/2333282

Koster, R. D., Mahanama, S. P. P., Livneh, B., Lettenmaier, D. P., & Reichle, R. H. (2010). Skill in streamflow forecasts derived from large-scale estimates of soil moisture and snow. *Nature Geoscience*, *3*(9), 613–616. https://doi.org/10.1038/ngeo944

Li, D., Wrzesien, M. L., Durand, M., Adam, J., & Lettenmaier, D. P. (2017). How much runoff originates as snow in the western United States, and how will that change in the future? *Geophysical Research Letters*, *44*(12), 6163–6172. https://doi.org/10.1002/2017GL073551

Liang, X., & Lettenmaier, D. (1994). a simple hydrologically based model of land surface water and energy fluxes for general circulation models. *Journal of Geophysical …*, *99*. Retrieved from http://onlinelibrary.wiley.com/doi/10.1029/94JD00483/full

Little, K., Kingston, D. G., Cullen, N. J., & Gibson, P. B. (2019). The Role of Atmospheric Rivers for Extreme Ablation and Snowfall Events in the Southern Alps of New Zealand. *Geophysical Research Letters*, *46*(5), 2761–2771. https://doi.org/10.1029/2018GL081669

Livezey, R. E., & Chen, W. Y. (1983). Statistical field significance and its determination by Monte Carlo techniques. *Monthly Weather Review*. https://doi.org/10.1175/1520-0493(1983)111<0046:SFSAID>2.0.CO;2

Livneh, B., Rosenberg, E. A., Lin, C., Nijssen, B., Mishra, V., Andreadis, K. M., et al. (2013). A long-term hydrologically based dataset of land surface fluxes and states for the conterminous United States: Update and extensions. *Journal of Climate*, *26*(23), 9384–9392. https://doi.org/10.1175/JCLI-D-12-00508.1

Mann, H. B. (1945). Nonparametric Tests Against Trend. *Econometrica*, *13*(3), 245. https://doi.org/10.2307/1907187

Margulis, S. A., Girotto, M., Cortés, G., & Durand, M. (2015). A Particle Batch Smoother Approach to Snow Water Equivalent Estimation. *Journal of Hydrometeorology*, *16*(4), 1752–1772. https://doi.org/10.1175/jhm-d-14-0177.1

Margulis, S. A., Cortés, G., Girotto, M., & Durand, M. (2016). A landsat-era Sierra Nevada snow reanalysis (1985-2015). *Journal of Hydrometeorology*, *17*(4), 1203–1221. https://doi.org/10.1175/JHM-D-15-0177.1

Maurer, E. P., Wood, A. W., Adam, J. C., Lettenmaier, D. P., & Nijssen, B. (2002). A Long-Term Hydrologically Based Dataset of Land Surface Fluxes and States for the Conterminous United States*. *Journal of Climate*, *15*(22), 3237–3251. https://doi.org/10.1175/1520-0442(2002)015<3237:ALTHBD>2.0.CO;2

McAfee, S. A., McCabe, G. J., Gray, S. T., & Pederson, G. T. (2019). Changing station coverage impacts temperature trends in the Upper Colorado River basin. *International Journal of Climatology*, *39*(3), 1517–1538. https://doi.org/10.1002/joc.5898

Mote, P. W., Hamlet, A. F., Clark, M. P., & Lettenmaier, D. P. (2005). Declining Mountain Snowpack in Western North America*. *Bulletin of the American Meteorological Society*, *86*(1), 39–49. https://doi.org/10.1175/BAMS-86-1-39

Mote, P. W., Li, S., Lettenmaier, D. P., Xiao, M., & Engel, R. (2018). Dramatic declines in snowpack in the western US. *Npj Climate and Atmospheric Science*, *1*(1), 2. https://doi.org/10.1038/s41612-018-0012-1

Painter, T. H., Deems, J. S., Belnap, J., Hamlet, A. F., Landry, C. C., & Udall, B. (2010). Response of Colorado river runoff to dust radiative forcing in snow. *Proceedings of the National Academy of Sciences of the United States of America*, *107*(40), 17125–17130. https://doi.org/10.1073/pnas.0913139107

Rasmussen, R., Liu, C., Ikeda, K., Gochis, D., Yates, D., Chen, F., et al. (2011). High-resolution coupled climate runoff simulations of seasonal snowfall over Colorado: A process study of current and warmer climate. *Journal of Climate*, *24*(12), 3015–3048. https://doi.org/10.1175/2010JCLI3985.1

Rosenberg, E. A., Clark, E. A., Steinemann, A. C., & Lettenmaier, D. P. (2013). On the contribution of groundwater storage to interannual streamflow anomalies in the Colorado River basin. *Hydrology and Earth System Sciences*, *17*(4), 1475–1491. https://doi.org/10.5194/hess-17-1475-2013

Rosenberg, Eric A., Wood, A. W., & Steinemann, A. C. (2013). Informing hydrometric network design for statistical seasonal streamflow forecasts. *Journal of Hydrometeorology*, *14*(5), 1587–1604. https://doi.org/10.1175/JHM-D-12-0136.1

Schneider, D., & Molotch, N. P. (2016). Real-time estimation of snow water equivalent in the Upper Colorado River Basin using MODIS-based SWE Reconstructions and SNOTEL data. *Water Resources Research*, *52*(10), 7892–7910. https://doi.org/10.1002/2016WR019067

Serreze, M. C., Clark, M. P., & Frei, A. (2001). Characteristics of large snowfall events in the montane western United States as examined using snowpack telemetry (SNOTEL) data. *Water Resources Research*, *37*(3), 675–688. https://doi.org/10.1029/2000WR900307

Timilsena, J., & Piechota, T. (2008). Regionalization and reconstruction of snow water equivalent in the upper Colorado River basin. *Journal of Hydrology*, *352*(1–2), 94–106. https://doi.org/10.1016/j.jhydrol.2007.12.024

Trujillo, E., & Molotch, N. P. (2014). Snowpack regimes of the Western United States. *Water Resources Research*, *50*(7), 5611–5623. https://doi.org/10.1002/2013WR014753

Vano, J. A., Das, T., & Lettenmaier, D. P. (2012). Hydrologic Sensitivities of Colorado River Runoff to Changes in Precipitation and Temperature*. *Journal of Hydrometeorology*, *13*(3), 932–949. https://doi.org/10.1175/JHM-D-11-069.1

Vano, J. A., Udall, B., Cayan, D. R., Overpeck, J. T., Brekke, L. D., Das, T., et al. (2014). Understanding Uncertainties in Future Colorado River Streamflow. *Bulletin of the American Meteorological Society*, *95*(1), 59–78. https://doi.org/10.1175/BAMS-D-12-00228.1

Wang, X., & Shen, S. S. (1999). Estimation of spatial degrees of freedom of a climate field. *Journal of Climate*, *12*(5 I), 1280–1291. https://doi.org/10.1175/1520-0442(1999)012<1280:EOSDOF>2.0.CO;2

Xiao, M., Udall, B., & Lettenmaier, D. P. (2018). On the causes of declining Colorado River streamflows. *Water Resources Research*, *2*, 1–18. https://doi.org/10.1029/2018WR023153

Yan, H., Sun, N., Wigmosta, M. S., Leung, L. R., Hou, Z., Coleman, A., & Skaggs, R. (2019). Evaluating next-generation intensity-duration-frequency curves for design flood estimates in the snow-dominated western United States. *Hydrological Processes*, (May), under review. https://doi.org/10.1002/hyp.13673

Table 1: Long-term mean number of storm days, all storms and AR-storms in one year as described in section 3.3. All-water year climatology is also provided for reference.

	Wet years	Dry years	Warm years	Cold years	All years
Storm days	54.9	23.0	36.2	41.5	37.4
All Storms	18.7	12.8	14.8	17.6	16.2
AR-storms	13.2	8.0	10.9	11.9	11.2

Table 2: Average contributions of AR-storm, all storms and all precipitation to annual peak SWE for wet, dry, warm and cold years. The last column presents the climatology of the basin annual SWE maximum under each category.

	Wet years	Dry years	Warm years	Cold years	All years
(a) AR-storm	65.9%	49.7%	61.7%	56.0%	56.9%
(b) All storms	86.1%	70.3%	84.0%	76.9%	78.2%
Total	107.1%	118.7%	119.8%	104.5%	110.6%
(a)/(b)	76.5%	70.7%	73.5%	72.8%	72.8%
SWE (km^3)	34.0	13.8	20.3	27.1	23.2
ΔSWE per AR-storm (km^3)	1.97	1.22	1.37	1.66	1.51
ΔSWE per storm (km^3)	1.57	0.76	1.15	1.18	1.12

Table 3: Percentage of grid cells that have trends in annual contribution of AR-storm, all storm and all precipitation (Total) at 0.05 significant level over the domain.

	AR-storm	All storm	Total
Upward trend	8.9%	16.1%	20.1%
Downward trend	8.0%	9.7%	11.2%

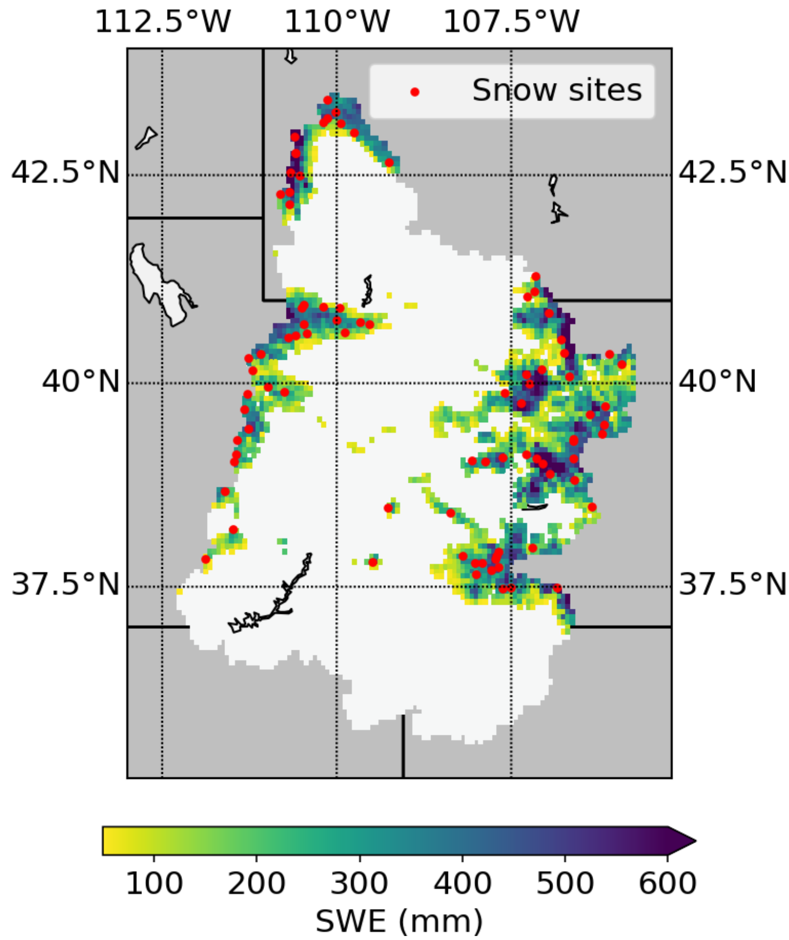

Figure 1: Headwater regions in the Upper Colorado River Basin. Only those grid cells with long-term average Apr 1st SWE>50mm are shown. Red dots mark the 86 SNOTEL station locations within the domain.

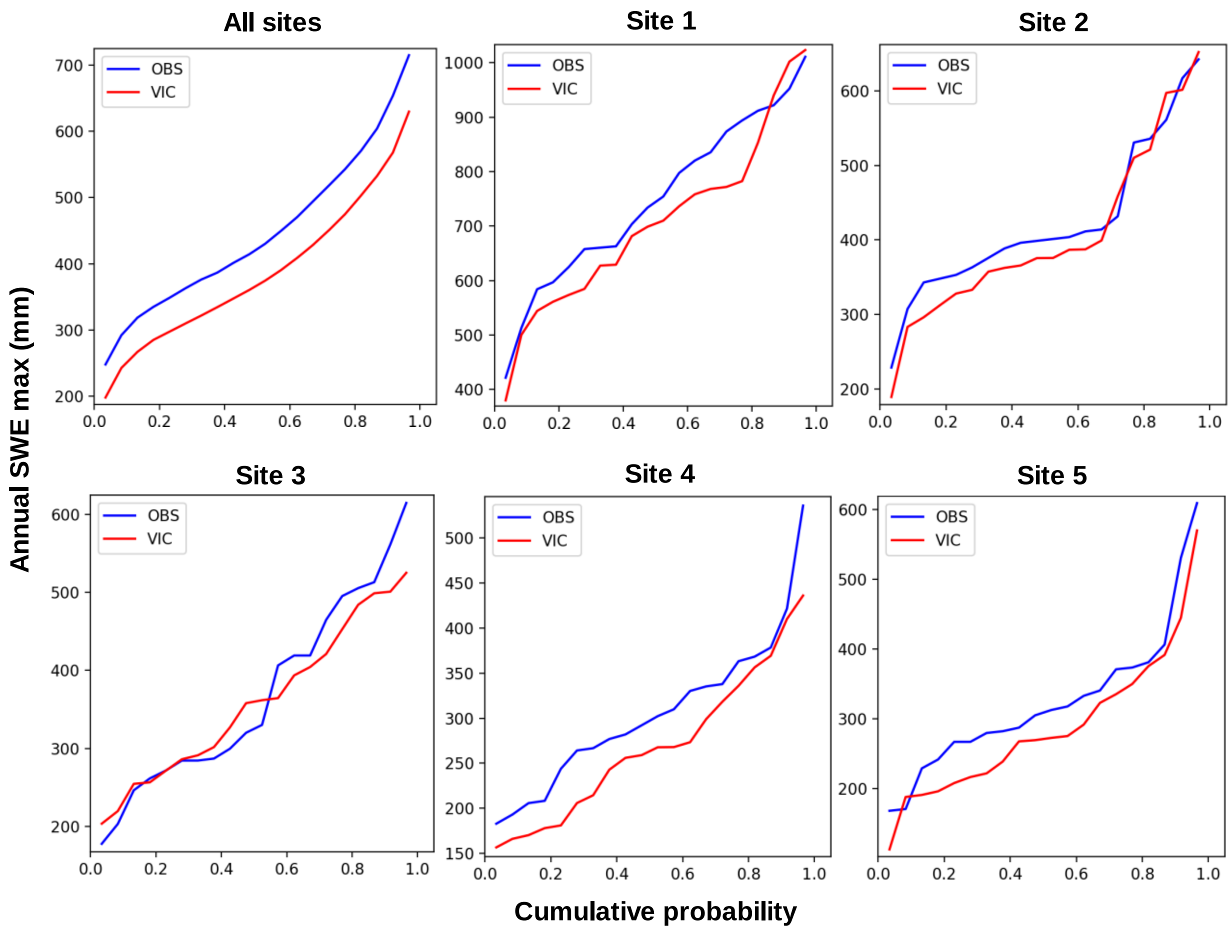

Figure 2: CDFs of simulated (red) and observed (blue) annual SWE maxima over 1991-2011. The first panel is the average result across all 86 SNOTEL sites. The other panels are for 5 selected stations (detailed information of these 5 sites is provided in the Figure S2 and Table S1 in the supplement).

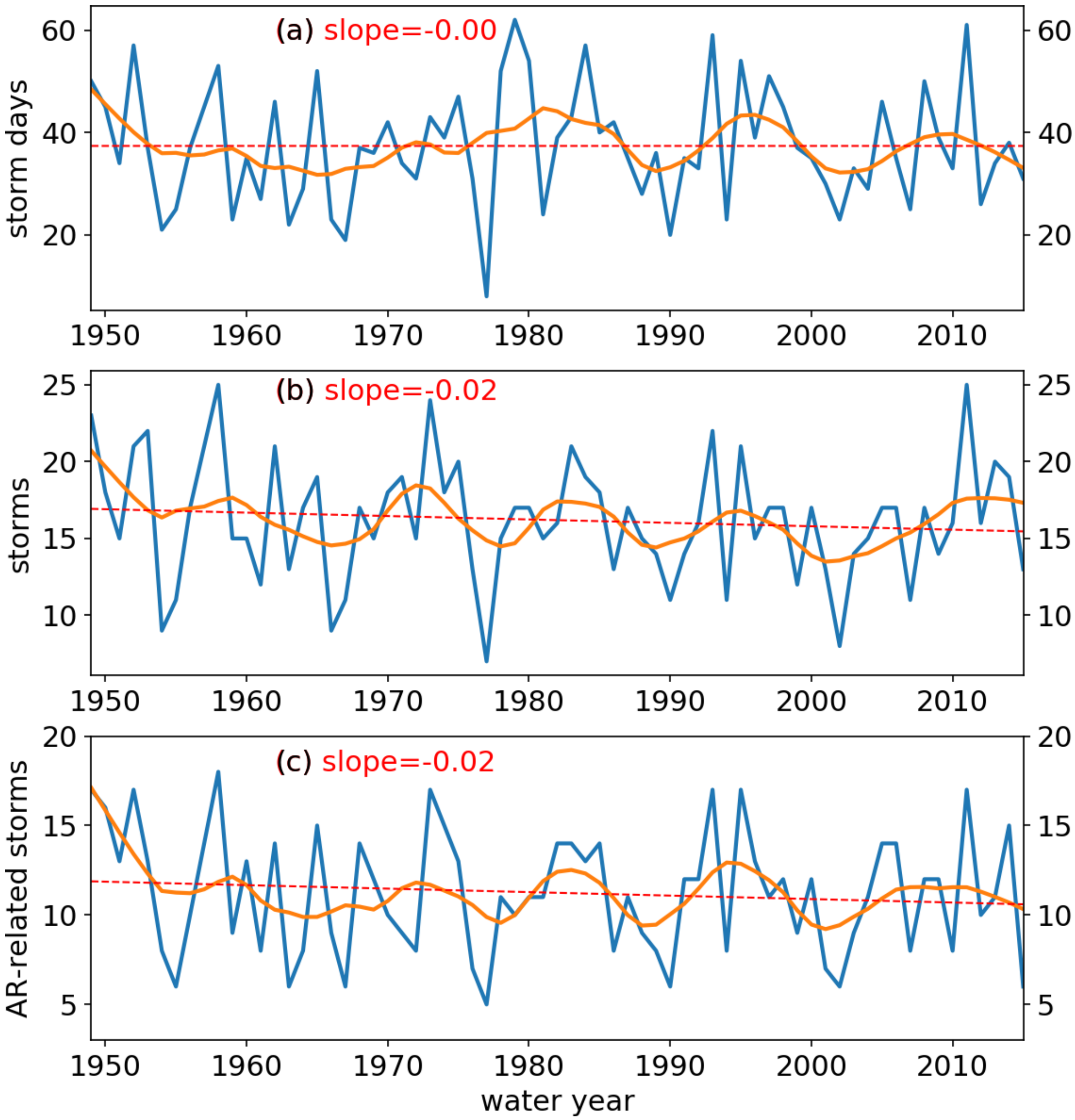

Figure 3: Time series of number of storm days (top), number of storms (middle) and number of AR-related storms (bottom) for 1949-2015. The red dashed line is the linear regression against time (although none is statistically significant). The slope is reported in red. The orange line is smoothed using a Lowess fitter (fraction = 0.17).

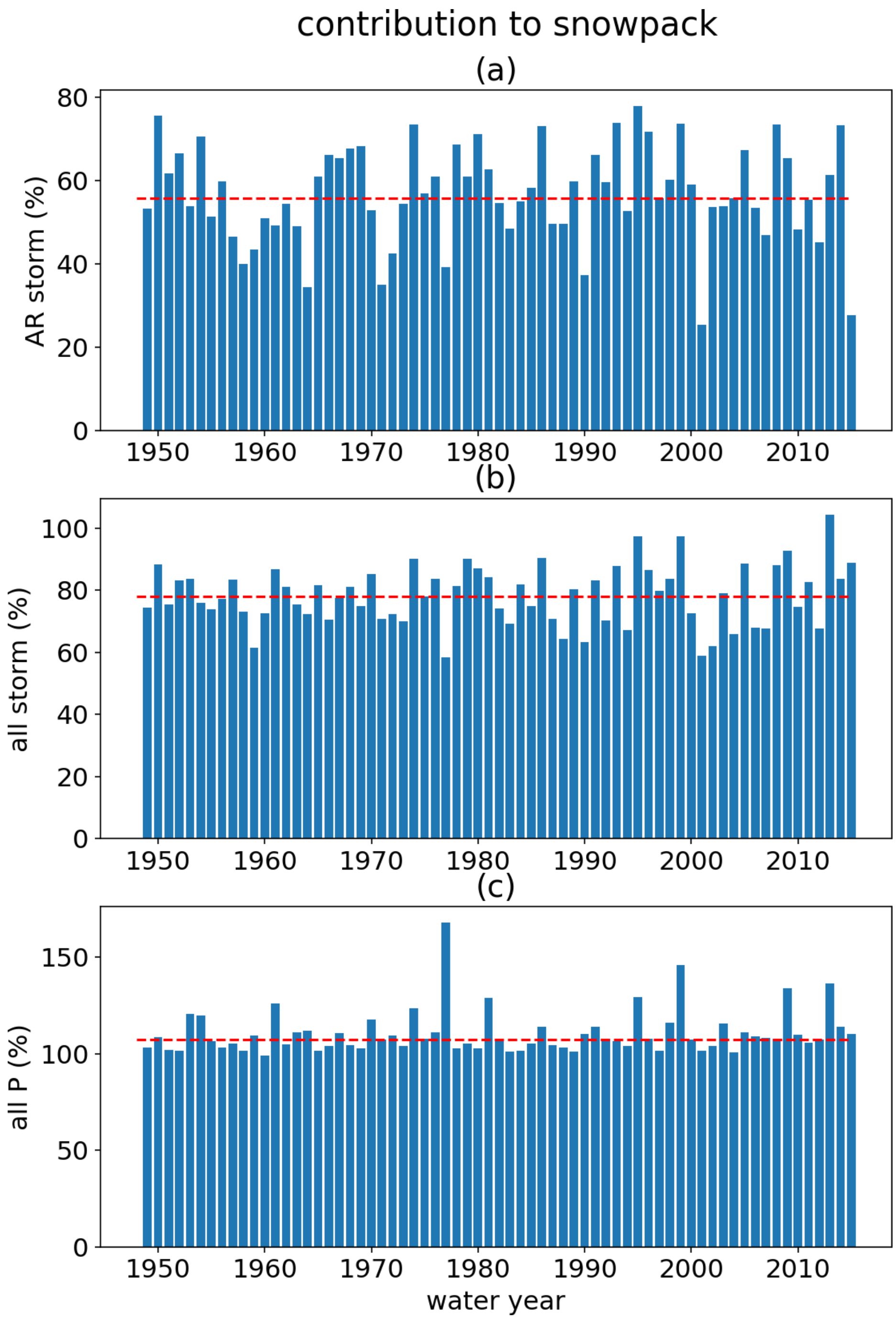

Figure 4: The contribution of (a) AR-storms, (b) all storms and (c) all precipitation to basin-wide SWE in each year. The red dashed line indicates the long-term mean.

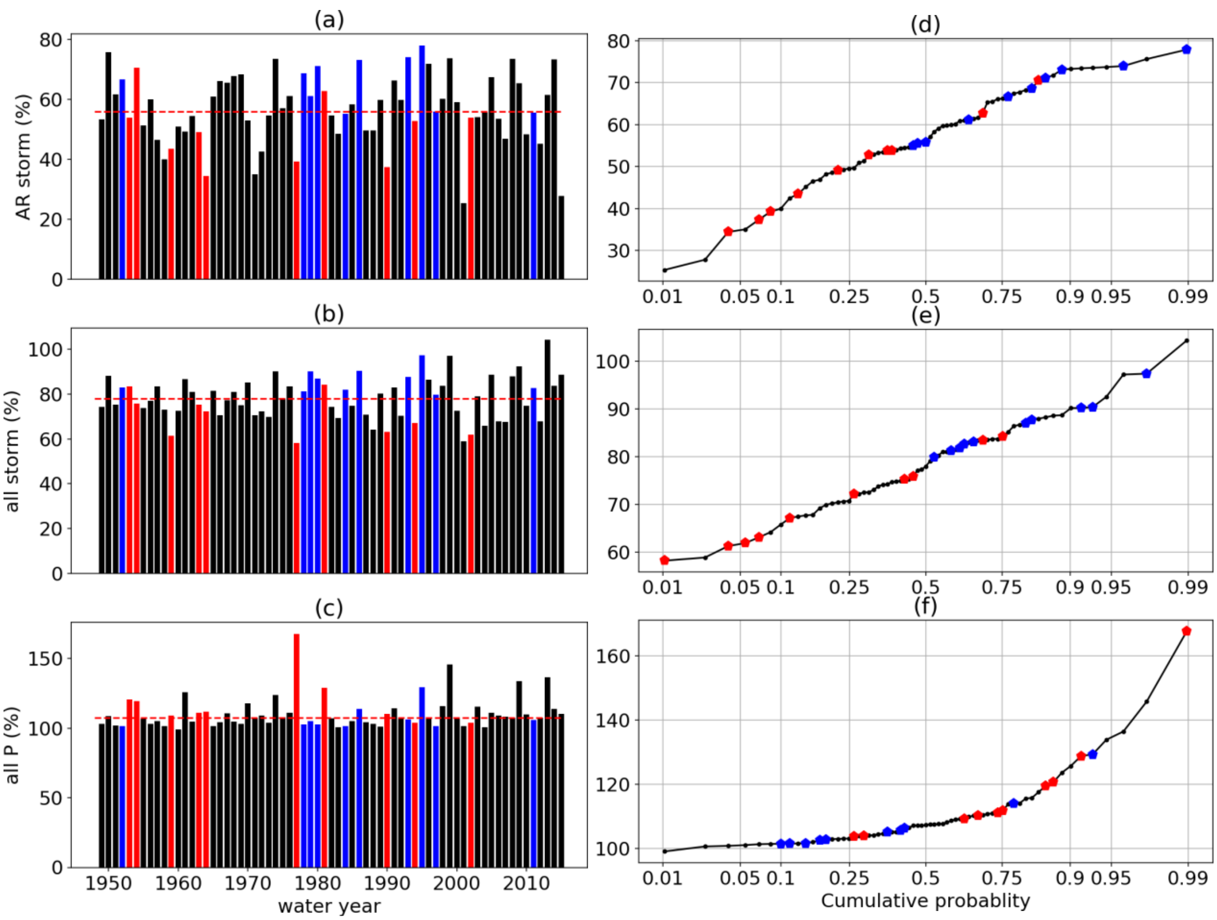

Figure 5: Bar plots (left column) and empirical distributions (right column) of the contribution to peak SWE of AR storms, all storms, and all precipitation over the study period. Wet years are highlighted with blue and dry years are with red. The left column bars are the same as in Figure 4.

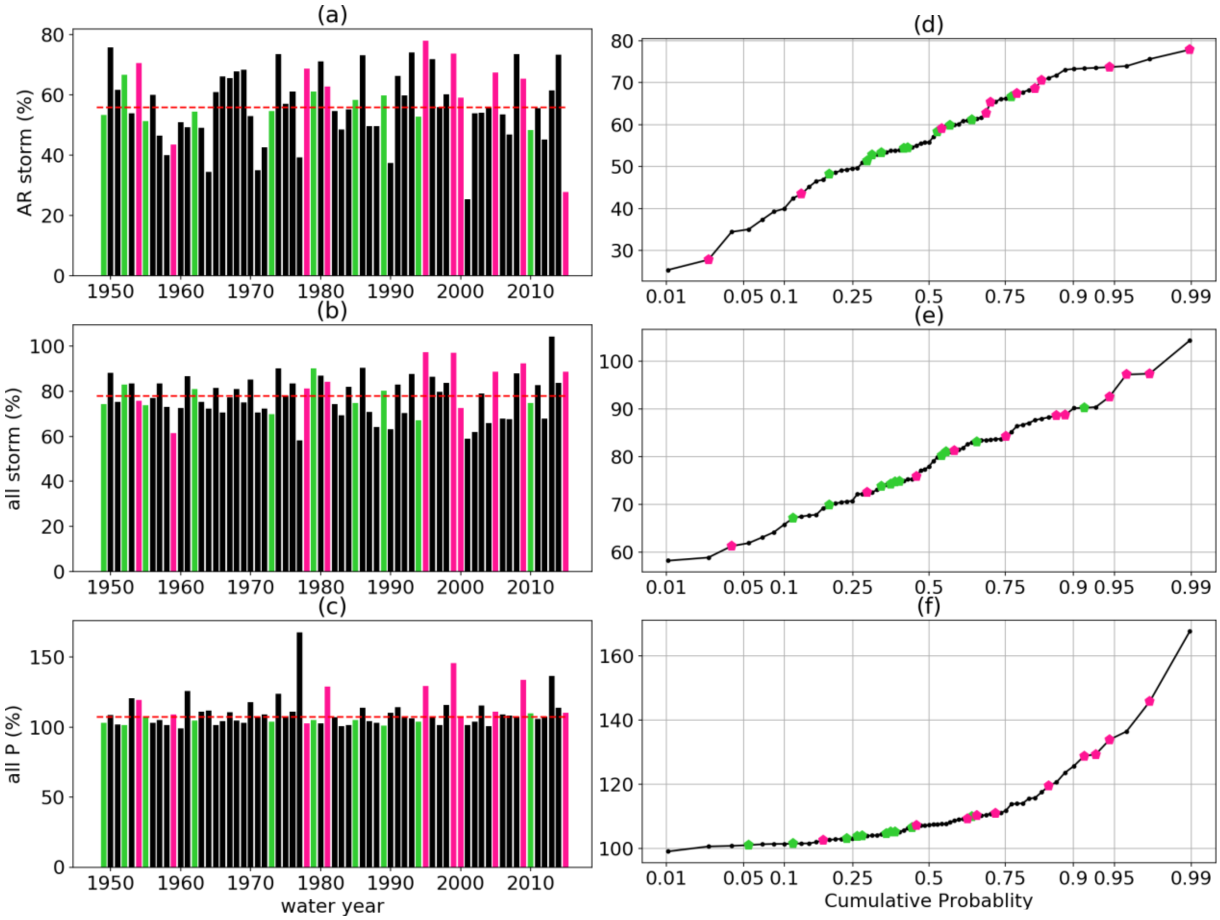

Figure 6: Same as Figure 5 but for warm years (pink) and cold years (green).

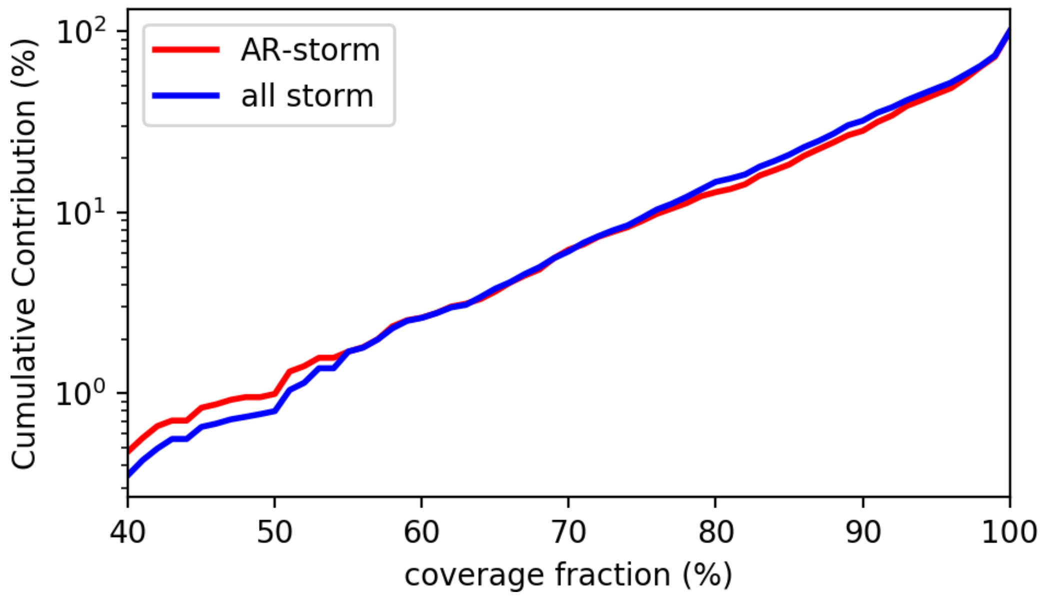

Figure 7: Coverage area fraction vs cumulative contribution to snowpack of AR-storms (red) and all storms (blue). The y-axis is in log scale.

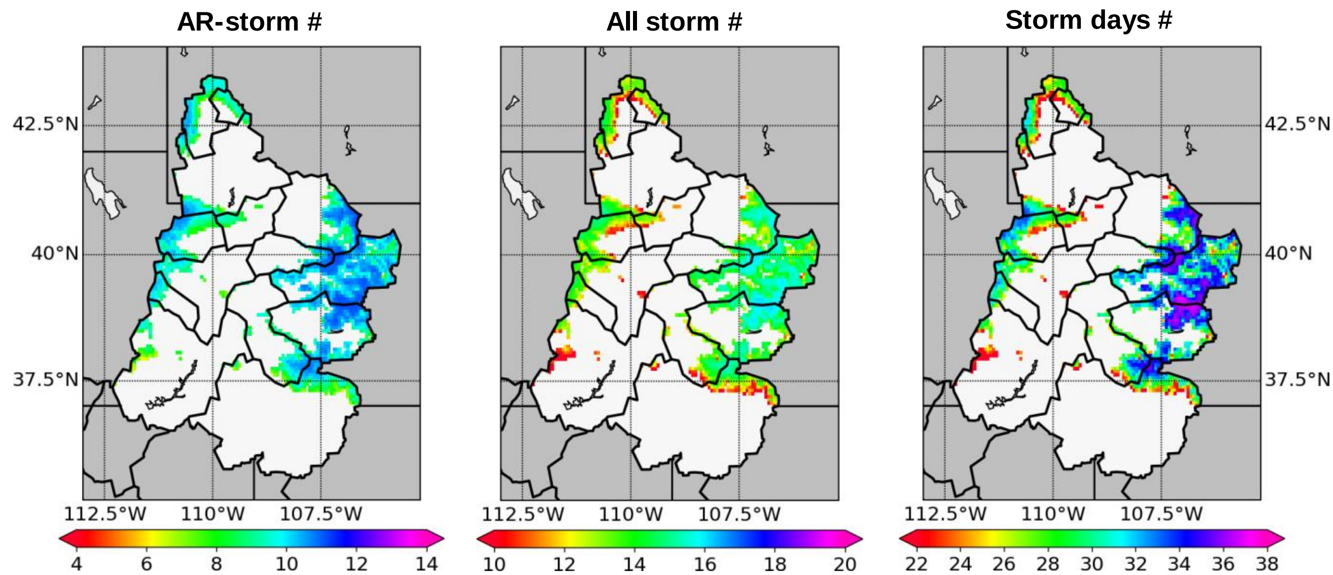

Figure 8: Multiyear average number of AR-storms (left), all storms (middle) and storm days (right) for all grid cells. Note that the color scales are different in each panel.

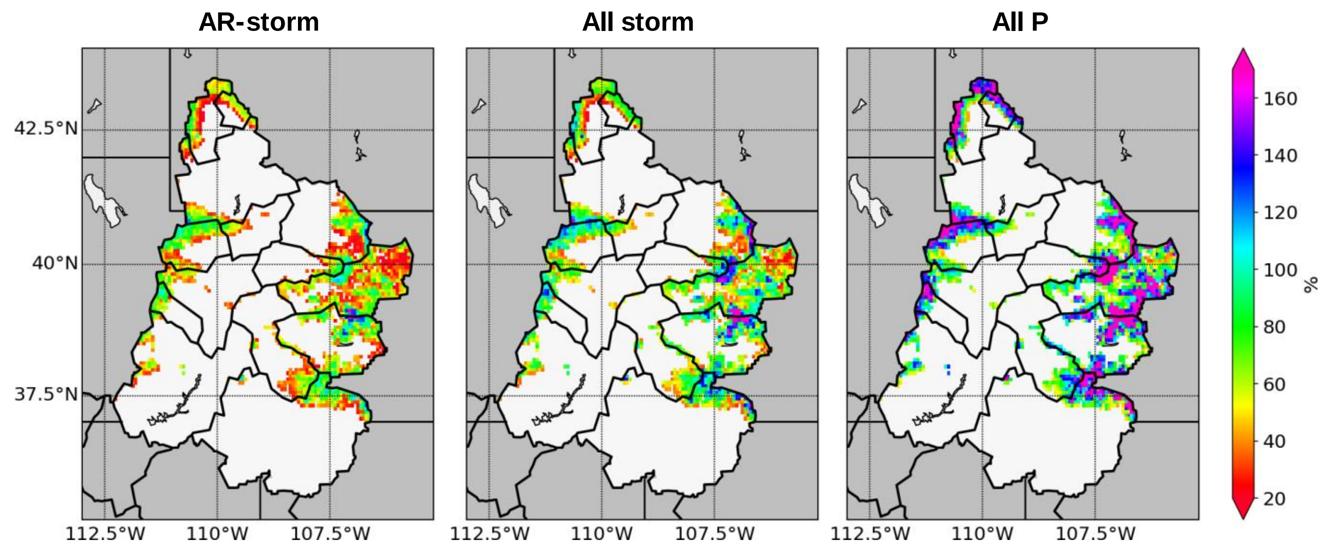

Figure 9: AR-storm (left), all storms (middle) and all precipitation (right) average contribution to annual SWE maximum over the 1949-2014 study period.

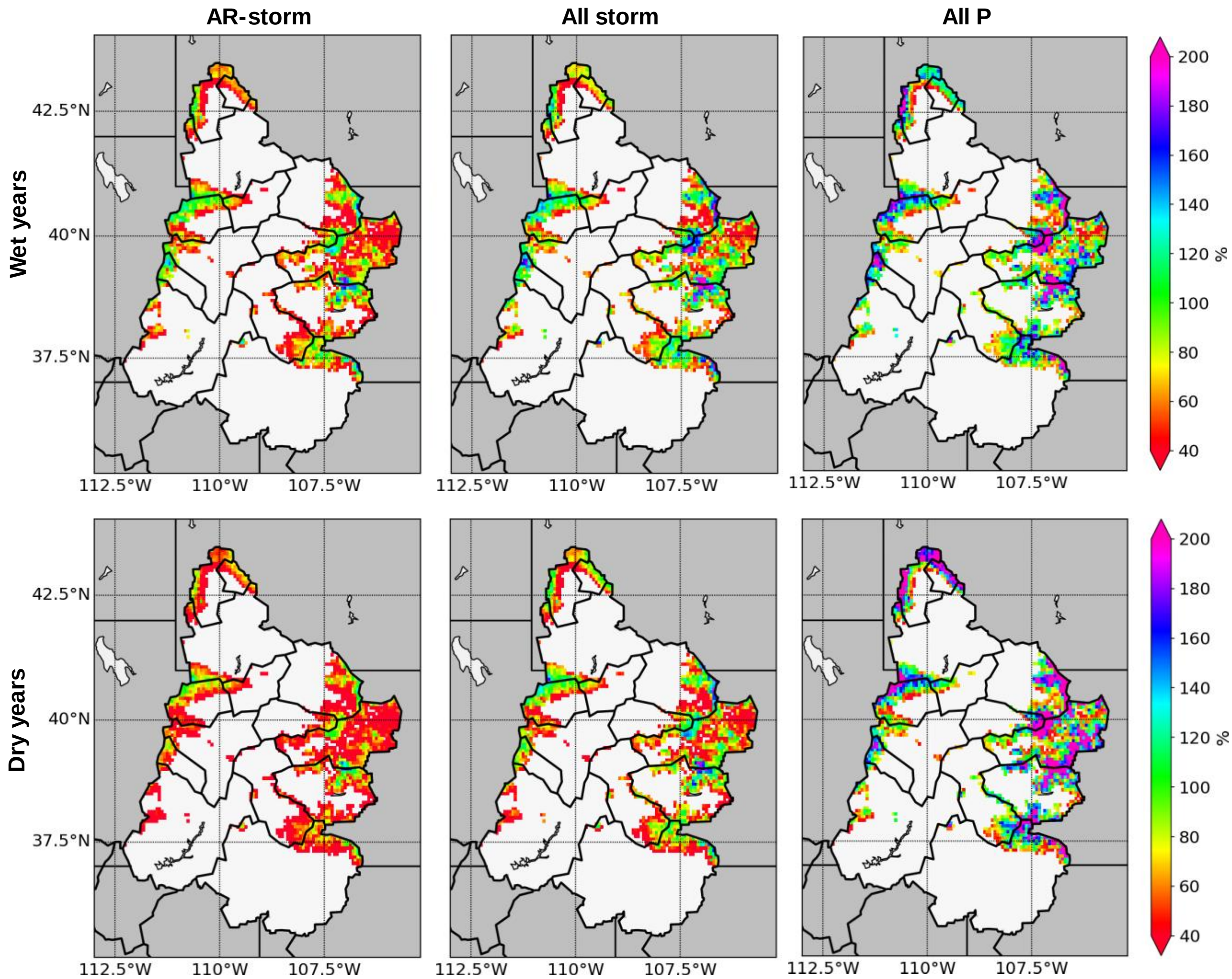

Figure 10: Average contribution of AR-storm, all storms and all precipitation to annual SWE maximum over the selected wet (top row) and dry (bottom row) years for each individual grid cell.

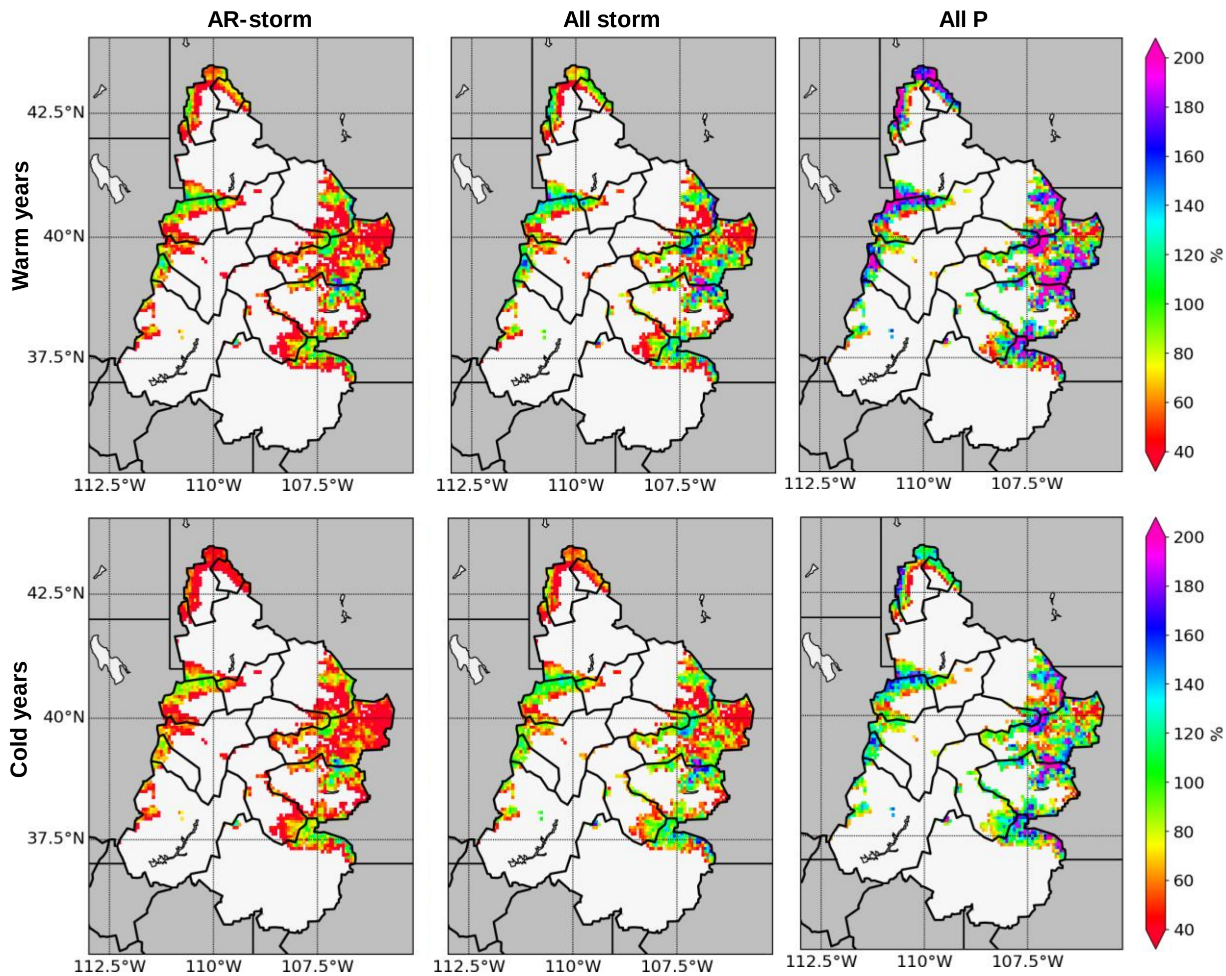

Figure 11: Same as Figure 9 but for warm (top row) and cold (bottom row) years.

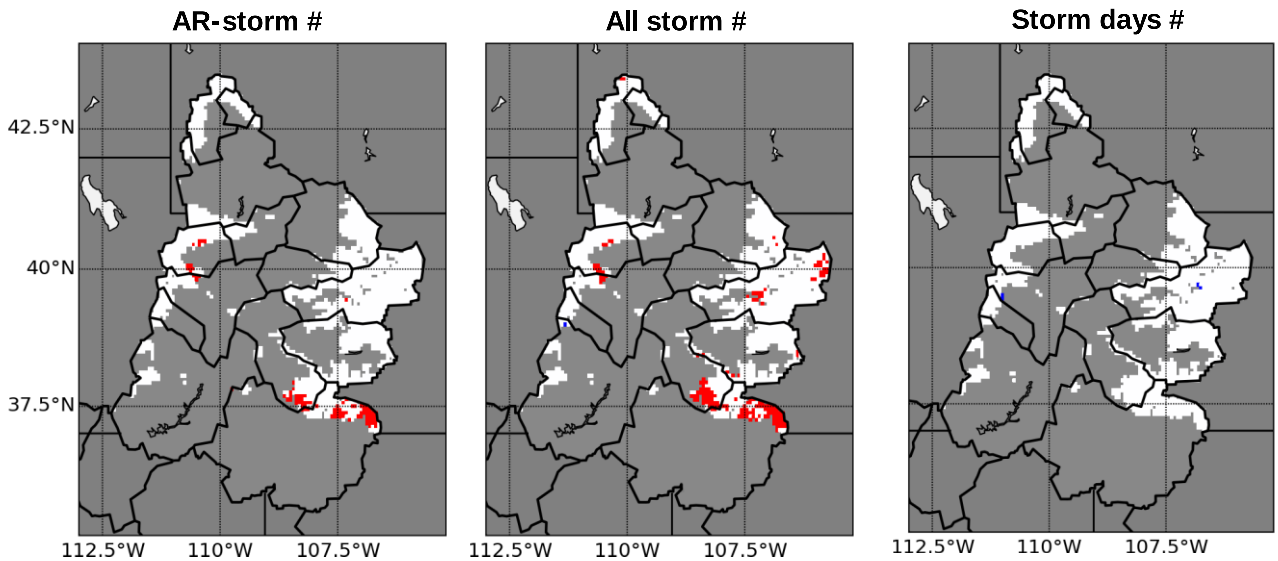

Figure 12: Annual trends (by MK-test at 0.05 significant level) in number of AR-storms (left), all storms (middle) and individual storm days (right) at all grid cells. Blue indicates upward trend, red is downward trend and white represents no significant trend. Only the grid cells with long-term Apr-1st SWE > 50 mm are shown.

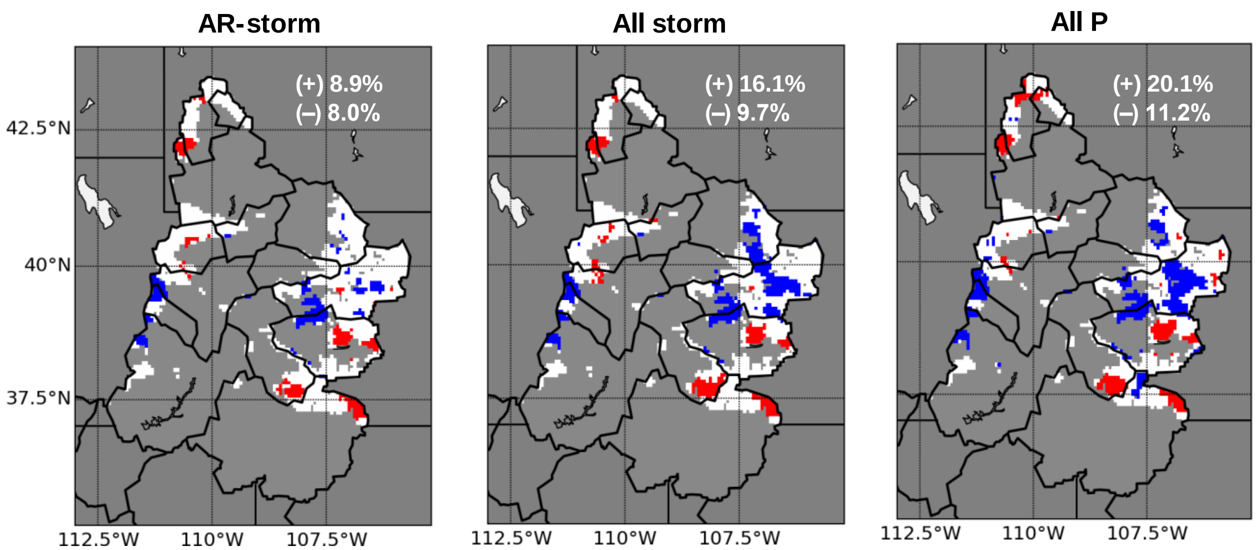

Figure 13: Annual trends (by MK-test at 0.05 significant level) in contributions of AR-storms (left), all storms (middle) and all precipitation (right) to annual maximum SWE. Blue indicates upward trend and red is downward trend.

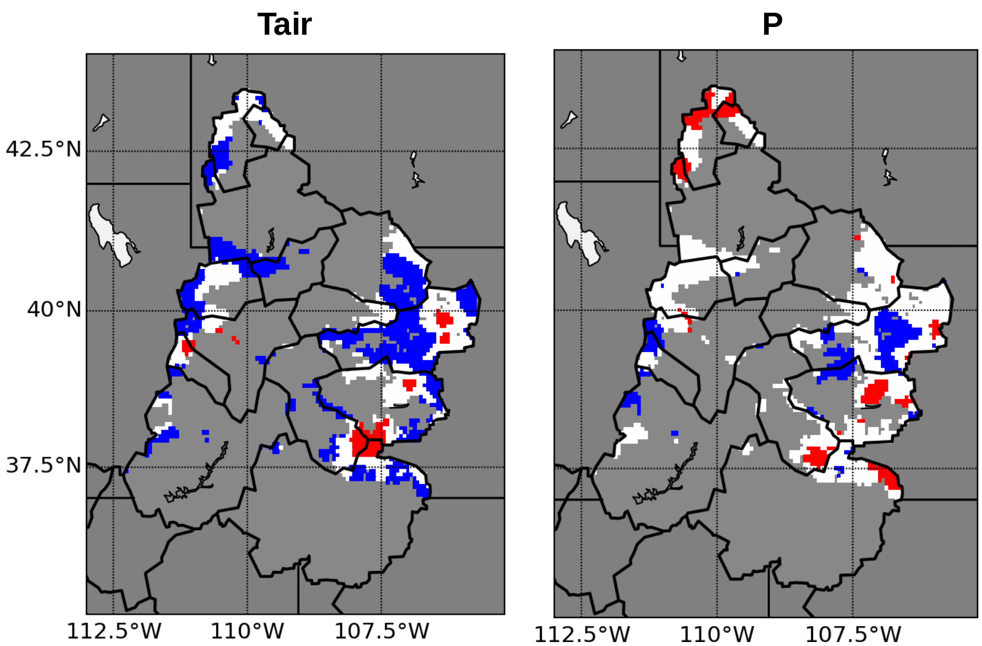

Figure 14: MK-trend test results for temperature (left) and total precipitation during the accumulation season at each single grid over the 1949-2015. Blue indicates statistically significant upward trend and red indicates statistically significant downward trend at 0.05 significance level.